Atmos. Chem. Phys., 15, 10799–10809, 2015
www.atmos-chem-phys.net/15/10799/2015/
doi:10.5194/acp-15-10799-2015

Atmospheric Chemistry and Physics
Open Access

The NO_x dependence of bromine chemistry in the Arctic atmospheric boundary layer

K. D. Custard[1], C. R. Thompson[1,5,b], K. A. Pratt[1,2], P B. Shepson[1,3], J. Liao[4,5,6], L. G. Huey[4], J. J. Orlando[7], A. J. Weinheimer[7], E. Apel[7], S. R. Hall[7], F. Flocke[7], L. Mauldin[7,a], R. S. Hornbrook[7], D. Pöhler[8], S. General[8], J. Zielcke[8], W. R. Simpson[9], U. Platt[8], A. Fried[11], P. Weibring[11], B. C. Sive[10], K. Ullmann[7], C. Cantrell[7,a], D. J. Knapp[7], and D. D. Montzka[7]

[1]Department of Chemistry, Purdue University, West Lafayette, IN, USA
[2]Department of Chemistry, University of Michigan, Ann Arbor, MI, USA
[3]Department of Earth, Atmospheric, and Planetary Sciences & Purdue Climate Change Research Center, Purdue University, West Lafayette, IN, USA
[4]School of Earth and Atmospheric Sciences, Georgia Institute of Technology, Atlanta, GA, USA
[5]Cooperative Institute for Research in Environmental Sciences, University of Colorado Boulder, Boulder, CO, USA
[6]Earth System Research Laboratory, National Oceanic and Atmospheric Administration, Boulder, CO, USA
[7]National Center for Atmospheric Research, Boulder, CO, USA
[8]Institute of Environmental Physics, University of Heidelberg, Heidelberg, Germany
[9]Geophysical Institute and Department of Chemistry, University of Alaska Fairbanks, Fairbanks, AK, USA
[10]National Park Service, Air Resources Division, Lakewood, CO, USA
[11]Institute of Arctic and Alpine Research, University of Colorado, Boulder, CO, USA
[a]now at: Atmospheric and Ocean Sciences, University of Colorado, Boulder, CO, USA
[b]now at: Chemical Sciences Division, National Oceanic and Atmospheric Administration, Boulder, CO, USA

Correspondence to: K. D. Custard (kcustard@purdue.edu)

Received: 8 January 2015 – Published in Atmos. Chem. Phys. Discuss.: 19 March 2015
Revised: 20 August 2015 – Accepted: 31 August 2015 – Published: 29 September 2015

Abstract. Arctic boundary layer nitrogen oxides ($NO_x = NO_2 + NO$) are naturally produced in and released from the sunlit snowpack and range between 10 to 100 pptv in the remote background surface layer air. These nitrogen oxides have significant effects on the partitioning and cycling of reactive radicals such as halogens and HO_x ($OH + HO_2$). However, little is known about the impacts of local anthropogenic NO_x emission sources on gas-phase halogen chemistry in the Arctic, and this is important because these emissions can induce large variability in ambient NO_x and thus local chemistry. In this study, a zero-dimensional photochemical kinetics model was used to investigate the influence of NO_x on the unique springtime halogen and HO_x chemistry in the Arctic. Trace gas measurements obtained during the 2009 OASIS (Ocean – Atmosphere – Sea Ice – Snowpack) field campaign at Barrow, AK were used to constrain many model inputs. We find that elevated NO_x significantly impedes gas-phase halogen radical-based depletion of ozone, through the production of a variety of reservoir species, including HNO_3, HO_2NO_2, peroxyacetyl nitrate (PAN), $BrNO_2$, $ClNO_2$ and reductions in BrO and HOBr. The effective removal of BrO by anthropogenic NO_x was directly observed from measurements conducted near Prudhoe Bay, AK during the 2012 Bromine, Ozone, and Mercury Experiment (BROMEX). Thus, while changes in snow-covered sea ice attributable to climate change may alter the availability of molecular halogens for ozone and Hg depletion, predicting the impact of climate change on polar atmospheric chemistry is complex and must take into account the simultaneous impact of changes in the distribution and intensity of anthropogenic combustion sources. This is especially true for the Arctic, where NO_x emissions are expected to increase because of increasing oil and gas extraction and shipping activities.

Published by Copernicus Publications on behalf of the European Geosciences Union.

1 Introduction

The episodic depletion of O_3 in the Arctic boundary layer following polar sunrise, referred to as ozone depletion events (ODEs), is attributed to a bromine gas phase reaction scheme, propagated by cycles such as Reactions (R1–R3; Simpson et al., 2007; McConnell et al., 1992).

$$Br_2 + h\nu \rightarrow 2Br \quad \text{(R1)}$$
$$2Br + 2O_3 \rightarrow 2BrO + 2O_2 \quad \text{(R2)}$$
$$BrO + BrO \rightarrow 2Br/Br_2 + O_2 \quad \text{(R3)}$$

Ambient measurements at various Arctic sites have revealed maximum BrO mixing ratios between 30 to 40 pptv in the springtime (Liao et al., 2012; Pohler et al., 2010). However, modeling studies have shown that heterogeneous chemistry at the surface is needed to facilitate enhanced reactive halogen levels and drive ODEs (Toyota et al., 2014; Thomas et al., 2012; Michalowski et al., 2000), and recent field observations demonstrated that Br_2 is photochemically produced within the surface snowpack (Pratt et al., 2013; Foster et al., 2001). This heterogeneous chemistry mechanism, known as the "bromine explosion", is dependent on reactions involving HO_x (Wennberg, 1999; Tang and McConnell, 1996; Vogt et al., 1996; Fan and Jacob, 1992) to produce hypohalous acids, which then oxidize halide ions at reactive surfaces (Huff and Abbatt, 2002; Abbatt, 1994).

$$BrO + HO_2 \rightarrow HOBr + O_2 \quad \text{(R4)}$$
$$HOBr \rightarrow HOBr_{(aq)} \quad \text{(R5)}$$
$$HOBr_{(aq)} + Br^-_{(aq)} + H^+_{(aq)} \rightarrow Br_{2(aq)} + H_2O \quad \text{(R6)}$$
$$Br_{2(aq)} \rightarrow Br_{2(g)} \quad \text{(R7)}$$

Although gas-phase halogen chemistry in the Arctic has now been studied for several decades (Impey et al., 1997; Hausmann and Platt, 1994; Barrie et al., 1988), few studies have examined the effect of atmospheric NO_x on these halogen chemical cycles. Model studies have shown that NO_x can react with halogen radicals through several reactions (as shown in Reactions R8–R12), to produce inorganic halogen nitrates or nitryl halides, which can, in turn, activate further halogen chemistry through heterogeneous reactions (Cao et al., 2014; Toyota et al., 2013; Morin et al., 2007, 2012; Thomas et al., 2012; Evans et al., 2003; Aguzzi and Rossi, 1999, 2002; von Glasow et al., 2002; Thorn et al., 1993), and thereby alter gas phase halogen radical reaction pathways.

$$XO + NO_2 \rightarrow XONO_2 \quad \text{(R8)}$$
$$XO + NO \rightarrow X + NO_2 \quad \text{(R9)}$$
$$X + NO_2 \rightarrow XNO_2 \quad \text{(R10)}$$
$$XONO_2 \rightarrow XONO_{2(aq)} \quad \text{(R11)}$$
$$XONO_{2(aq)} + H_2O \rightarrow HOX + HNO_3 \quad \text{(R12)}$$

Reaction (R8) can directly influence the bromine explosion, as lab studies have shown that gas phase $BrONO_2$ can hydrolyze on acidic surfaces to form HOBr, as shown in Reaction (R12) where X = Br (Hanson, 2003; Aguzzi and Rossi, 2002; Hanson et al., 1996). Thus, while reactions involving NO_x can terminate the gas phase radical chain reaction, they can also generate products that contribute to the bromine explosion. Thus, it is not intuitively obvious what impact(s) NO_x ultimately has on halogen chemistry. These halogen reaction pathways are summarized in Fig. 1 (Abbatt et al., 2012; Grannas et al., 2007; Simpson et al., 2007). As illustrated in Fig. 1, elevated levels of NO_x can impact the halogen cycle through a variety of reactions. However, the sensitivity of the halogen radical chain reaction to NO_x is currently not well understood.

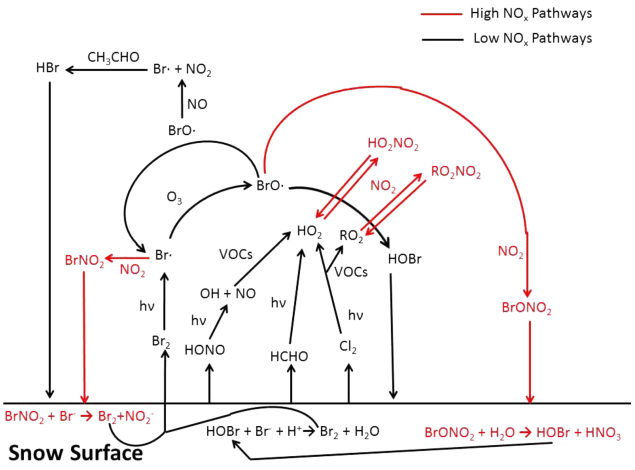

Figure 1. Halogen cycle in the Arctic boundary layer with (red trace) and without (black trace) the influence of anthropogenic NO_x (Abbatt et al., 2012; Simpson et al., 2007; Grannas et al., 2007).

The Arctic boundary layer typically has ambient background levels of NO_x between 10 to 100 pptv resulting from its isolation from major anthropogenic sources, with its primary sources being photochemical production within the snowpack (Villena et al., 2011; Honrath et al., 2002; Ridley et al., 2000), and long range transport of photolyzable species such as organic nitrates (Muthuramu et al., 1994). Arctic field studies have led to observations of NO_x fluxes from sun-lit snow surfaces (Grannas et al., 2007; Ridley and Orlando, 2003; Beine et al., 2002; Honrath et al., 1999, 2002), and lab studies have demonstrated that frozen solutions of nitrate and nitrite can release NO_x when irradiated with UV light (Dubowski et al., 2002, 2001; Honrath et al., 2000).

$$NO_3^- + h\nu \rightarrow NO_2 + O^- \quad \text{(R13)}$$
$$NO_2^- + h\nu \rightarrow NO + O^- \quad \text{(R14)}$$

With the possibility of increased anthropogenic sources throughout the Arctic, e.g. from coastal development, shipping, and oil and gas exploration, the impacts of increased NO_x are likely to be seen (Peters et al., 2011; Corbett et al., 2010). However, the snow surface is an extremely complex

matrix in which significant condensed phase photochemistry occurs, that we currently do not understand well and therefore can't properly simulate. Given the opportunity provided by the existing observational data base, we chose to investigate the effect of varying NO_x mixing ratios on gas phase Arctic halogen radical chemistry, using a zero-dimensional (0-D) photochemical model. The model is constrained by recent observations of a wide variety of relevant precursors and intermediates, during the OASIS 2009 campaign conducted at Barrow, AK. To complement the model studies, observational evidence of the impact of NO_x on BrO is examined from aircraft measurements near Prudhoe Bay, AK during the 2012 BROMEX.

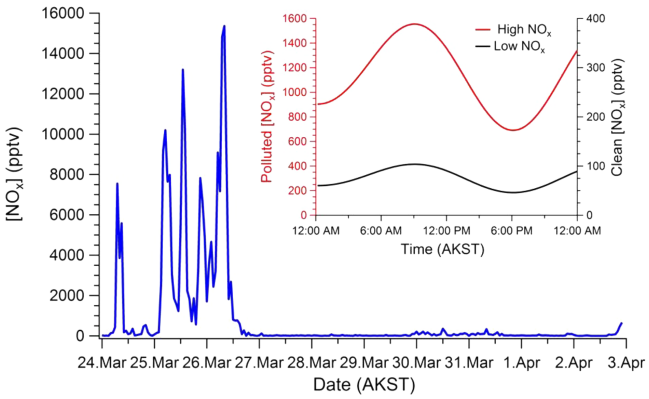

Figure 2. Observed (blue) NO_x mixing ratios for the 10-day OASIS period in Barrow, AK, as well as model scenario diurnal NO_x mixing ratios for low (black) and high (red) cases.

2 Model description

A 0-D photochemical model was developed using the modeling software FACSIMILE. The model has been described in detail by Thompson et al. (2015) and is described briefly here. The model includes known Arctic gas-phase chemistry with 189 gas-phase reactions (Table S1 in the Supplement) and 28 photolysis reactions (Table S2). The deposition of 19 gas-phase species to aerosols/snow surfaces (Table S3) and 16 aqueous-phase chemical reactions (Table S4) are also included, where the heterogeneous reactions are treated as aqueous reactions. The model is constrained to observations with time varying mixing ratios for a list of gas-phase species (Table S5), including halogen radical precursors (Cl_2 and Br_2) and a wide range of volatile organic compounds (C_2H_2, C_2H_4, C_2H_6, C_3H_8, C_3H_6, $n-C_4H_{10}$, i-C_4H_{10}, HCHO, CH_3CHO, CH_3COCH_3, and methyl ethyl ketone), as well as calculated, time varying photolysis rates, from the field study OASIS (Ocean – Atmosphere – Sea Ice – Snowpack) in Barrow, AK. Mixing ratios of selected gas-phase species along with the photolysis rates were called into the model every 10 min within the simulation. For this model study, the 10-day period from 24 March–2 April 2009 during OASIS 2009 was simulated. During this period, a 3-day ozone depletion event ($O_3 < 5$ ppbv) occurred, followed by a full ozone recovery ($O_3 > 20$ ppbv) that was due to vertical mixing (discussed in Sect. 3.1), and thus, covers a full range of typical atmospheric and meteorological conditions. It should be noted that the constrained mixing ratio for Br_2 on 30 and 31 March in the model is based on the observed diurnal average of 29 March and 1 April. As discussed in Liao et al. (2012) atmospheric observations for Br_2 on 30 and 31 March were not available.

To investigate the role that atmospheric NO_x plays in Arctic halogen chemistry, two different NO_x simulation scenarios were performed. A "low NO_x" case and a "high NO_x" case were used to create the two different scenarios. This allowed us to isolate a single variable between the two simulations. However, this approach does not consider other chemical species (i.e. VOCs (volatile organic compounds)) that could also be elevated along with anthropogenic NO_x. The two diurnal-cycle NO_x profiles were derived from the actual observed NO_x over the time period being simulated, as shown in Fig. 2. Representative average polluted (high) and clean (low) NO_x diurnal cycles, which differ by about a factor of 15, were calculated based on observed local NO_x mixing ratio data for the period (Fig. 2). The clean (low NO_x) and polluted (high NO_x) days during the 10 day (24 March to 2 April) period studied were selected based on the work of Villena et al. (2011), in which correlations with ambient CO enhancements were used to identify air masses influenced by local emissions, i.e. for conditions when [CO] > 160 ppbv. The non-influenced/background days were averaged together to calculate a "low NO_x" diurnal average that ranged between 50 to 100 pptv. These values were in the range of previous observations of background NO_x mixing ratios (Villena et al., 2011; Honrath et al., 2002; Ridley et al., 2000). The same was done for the days influenced by local anthropogenic emissions, to create the "high NO_x" diurnal average characterized by NO_x mixing ratios from 700 to 1600 pptv. Each diurnal average was fit to a sine wave curve to generate temporally smoothed profiles. During the 10-day simulation either the Low NO_x or High NO_x diurnal average was applied to each day of the simulation, to generate the two distinct model scenarios. This allowed us to evaluate the NO_x dependence of the chemistry, since it was the only parameter altered between the two scenarios.

Molecular halogens respond to changes in the deposition rates and condensed-phase chemistry, the latter of which cannot be well simulated given the current state of knowledge of physical and chemical processes occurring in the snowpack (Domine et al., 2013). Therefore, to ensure proper representation of the gas phase halogen chemistry, the atmospheric molecular halogen (Br_2 and Cl_2) mixing ratios were constrained to observations. The observations for these species reflect the impact of NO_x-dependent production of reactive reservoir species, and the impact of their deposition to and

chemistry within the snowpack. While the model was constrained to observations for stable species (Table S5), it was used to calculate various radical species' (e.g., BrO and Br) mixing ratios given the sources and sinks of these radicals. In this way, we calculate the effective NO_x-dependence of the gas-phase radical chemistry and the rate of ozone depletion, as discussed below.

3 Results

3.1 Bromine chain length

The chain length for a radical chain reaction is the rate of propagation divided by the rate of termination (or initiation). A chain length of < 1 means that most of the radicals terminate after production. Here we calculate the bromine radical chain length (Φ) for the interconversion of Br and BrO radicals using Eq. (1; Thompson et al., 2015) for the 10-day simulation, where k corresponds to the reaction rate of the associated species.

$$\Phi = \frac{\left(\begin{array}{c} 2k[\mathrm{BrO}]^2 + k[\mathrm{BrO}][\mathrm{ClO}] + k[\mathrm{BrO}][\mathrm{CH_3OO}] + k[\mathrm{BrO}][\mathrm{OH}] + \\ k[\mathrm{BrO}][\mathrm{O(^3P)}] + k[\mathrm{BrO}][\mathrm{CH_3COOO}] + k[\mathrm{BrO}][\mathrm{NO}] + J[\mathrm{BrO}] \end{array}\right)}{\left(\begin{array}{c} k[\mathrm{Br}][\mathrm{HO_2}] + k[\mathrm{Br}][\mathrm{C_2H_2}] + k[\mathrm{Br}][\mathrm{C_2H_4}] + k[\mathrm{Br}][\mathrm{C_3H_6}] + k[\mathrm{Br}][\mathrm{HCHO}] + \\ k[\mathrm{Br}][\mathrm{NO_2}](0.15) + k[\mathrm{Br}][\mathrm{CH_3CHO}] + k[\mathrm{Br}][\mathrm{C_3H_6O}] + k[\mathrm{Br}][\mathrm{C_4H_8O}] + \\ k[\mathrm{Br}][\mathrm{CH_3OOH}] + k[\mathrm{BrO}][\mathrm{HO_2}] + k[\mathrm{BrO}][\mathrm{CH_3OO}] + k[\mathrm{BrO}][\mathrm{C_3H_6}] + \\ k[\mathrm{BrO}][\mathrm{NO_2}] \end{array}\right)} \quad (1)$$

Termination reactions include those that form non-radical brominated species (e.g., HBr, HOBr, $BrONO_2$), with photochemical lifetimes substantially longer than that of BrO or Br. It should be noted that although production of certain species represents a termination of the gas phase Br chain reaction (e.g. HOBr and $BrONO_2$), they can also play a crucial role in producing and increasing the Br radicals available for reacting with ozone, either through photolysis or heterogeneous reactions. This emphasizes the complexity of the BrO_x cycle that takes place in the Arctic. In Eq. (1) the Br + NO_2 reaction is multiplied by the branching ratio (0.15) for the production of $BrNO_2$ (Orlando and Burkholder, 2000). Orlando and Burkholder (2000) observed that the dominant product for NO_2 reaction with a Br atom is BrONO, and while at lower temperatures isomerization to $BrNO_2$ is possible, the overall yield would still be minor. The production of BrONO is not considered a sink for BrO_x because of its rapid thermal decomposition, photolysis and reaction with Br radicals, regenerating BrO_x (Burkholder and Orlando, 2000; Orlando and Burkholder, 2000). The bromine chain length was only calculated during daylight hours (10:00 to 18:00 AKST) because the bromine radical chain is photochemically initiated via the photolysis of Br_2 (Reaction R1). The bromine radical chain length was calculated throughout the entire 10-day simulation for both the low and high NO_x simulations, as shown in Fig. 3.

Both the low NO_x and high NO_x simulations show a chain length dependence on ozone mixing ratio (Fig. 3), with generally higher chain lengths at high O_3, due to Reaction (R2). When the O_3 mixing ratio is > 5 ppbv, the average low NO_x bromine chain length was 1.72 (±0.70), while the average high NO_x bromine chain length was 1.81 (±0.35). The shorter simulated bromine chain lengths (< 1.0) on 26, 27, 28, and 31 March can be explained by the low O_3 mixing ratio (< 5 ppbv). One might hypothesize that the high NO_x simulation would yield a shorter bromine chain length because NO_x acts as a sink for BrO_x. Indeed, the model simulation shows that NO_x, on a percentage basis, is a more dominant sink for BrO_x during the high NO_x simulation compared to the low NO_x simulation (Fig. 4). However, during the low NO_x simulation the HO_2+BrO reaction significantly decreases the bromine chain length, occurring more frequently, by a factor of 170, compared to the high NO_x simulation. This is due to the suppression of HO_2 in the high NO_x simulation via Reactions (R15) and (R16).

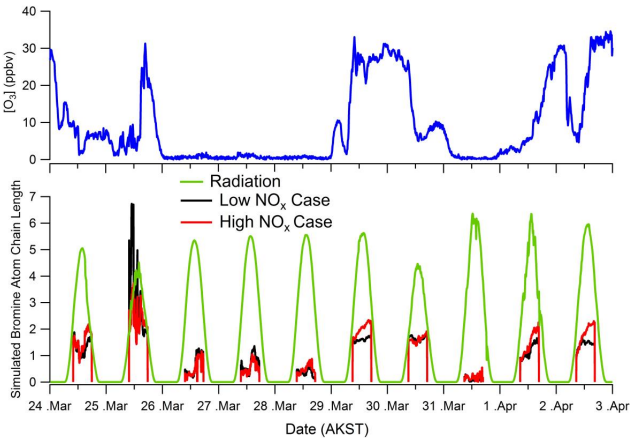

Figure 3. Calculated bromine chain length for the low NO_x simulation and the high NO_x simulation along with observed O_3 and radiation.

$$NO + HO_2 \rightarrow NO_2 + OH \quad (R15)$$

$$OH + NO_2 \rightarrow HNO_3 \quad (R16)$$

One point of interest is the much larger bromine chain length on 25 March, when ozone was partially depleted (< 15 ppbv), compared to other days with partially depleted ozone (30 March and 1 April). On this day a very large NO_x plume (∼ 15 ppbv) from the town of Barrow was observed compared to the relatively low NO_x conditions observed on 30 March and 1 April. Two important terms in the chain length for this day are $2k[BrO]^2$ and k[BrO][NO]. For this day, both [BrO] and [NO] are elevated (Figs. 2 and 7a). The rate of Reaction (R3) is quadratic in BrO mixing ratio, and, as discussed by Thompson et al. (2015), and indicated in Eq. (1), the observed chain length increases with BrO mixing ratio.

3.2 Net O_3 loss rate

Although the bromine chain length is relatively unchanged between the two scenarios, high levels of NO_x decrease the rate of net O_3 loss within the model. The net O_3 loss rate

was calculated from Eq. (2) as the sum of all of the rates of the chemical reactions that destroy ozone minus the sum of the rates of the chemical reactions that produce ozone (Thompson et al., 2015). It should be noted that the reactions in Eq. (2) that produce ozone (the 6th through 9th terms of the equation) are included as offsets for the depleted ozone destruction rate, which includes XO photolysis and NO oxidation to NO_2.

$$\text{Net } O_3 \text{ Loss Rate} = \left(\begin{array}{c} k[Br][O_3] + k[Cl][O_3] + k[O(^1D)][H_2O] + k[OH][O_3] + \\ k[HO_2][O_3] - k[BrO][NO] - J[BrO] - k[ClO][NO] - J[ClO] \end{array} \right) \quad (2)$$

Reaction counters were utilized for all the HO_2/RO_2+ NO reactions for both NO_x scenarios to determine the importance of those reactions towards O_3 production. The two different NO_x cases yielded equal numerical values when the counters were summed, indicating that NO_x did not have a large impact on these small O_3 production terms. The calculated net O_3 loss rate for both NO_x scenarios is shown in Fig. 5. On average, the net O_3 loss rate is a factor of 2 times slower for the high NO_x simulation compared with the low NO_x simulation. This can be explained by decreased BrO_x during the high NO_x simulation compared to the low NO_x simulation in significant part due to the enhancement in the rate of Reaction (R10), as shown in Fig. 4. To study this effect further, we calculated the net O_3 destruction rate as a function of NO_x mixing ratio by conducting simulations with a wide range of NO_x mixing ratios. The various NO_x diurnal cycles were calculated by starting with the low NO_x diurnal profile and step-wise increasing the NO_x by 250 pptv until the diurnal maximum of 2000 pptv was reached. The results, for the period 11:00–13:00 on 30 March are shown in Fig. 6. 30 March was selected because it fell into the "clean day" category during OASIS and during a time when ozone was decreasing from 30 to 5 ppbv. As shown in Fig. 6, the net O_3 loss rate decreases steeply, by a factor of 1.5 (from 0.80 to 0.52 ppbv hr^{-1}), during the increase of NO_x mixing ratios of ∼ 100–500 pptv, clearly expressing the strong NO_x-dependence of the chain reaction. We note, however, that this model experiment is directly testing the gas-phase component of this sensitivity on NO_x, and not the NO_x dependence of $BrONO_2$ deposition. However, as discussed later, when NO_x increases, BrO decreases and thus $BrONO_2$ is not sensitive to the NO_x mixing ratio. This does not negate the potential importance of $BrONO_2$ during ODEs. Cao et al. (2014) found, from a modeling study, that $BrONO_2$ production increased the rate of ozone depletion through the production of HOBr from its hydrolysis (Reaction R12) on snow/aerosol surfaces. HOBr is a main component of the bromine explosion and leads to an increased production rate of Br_2 (Reactions R5–R6). However, regression of the observed [Br_2] vs. observed [NO_x] reveals that the highest mixing ratios of Br_2 do in fact occur when NO_x is below 300 pptv (Fig. S1 in the Supplement). This is likely due to the fact that HO_2 is high when NO_x is low, contributing to greater HOBr at low NO_x (see Fig. 7b for HOBr on this day). This observed Br_2 clearly

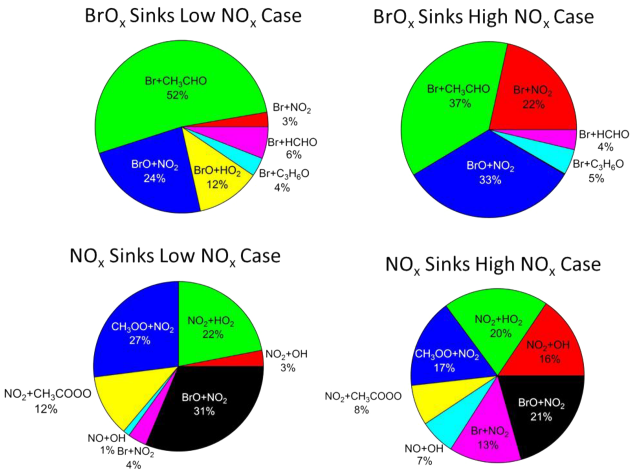

Figure 4. Fractional contributions of BrO_x and NO_x sink reactions from the low and high NO_x simulation cases (Note that Br+NO_2 only represents $BrNO_2$ production).

supports that the O_3 loss rate is minimized when NO_x mixing ratios are elevated, as the maximum Br atom production rates will occur at low [NO_x]. The net ozone loss is, of course, also extremely low for days when the observed mixing ratios of O_3 were very small (< 5 ppbv), as the rate of ozone destruction will approach zero as O_3 is nearly completely removed. Based on the results from Figs. 5 and 6, the influence that elevated NO_x mixing ratios have on decreasing the net ozone loss rate could be a factor in the Arctic as NO_x point sources continue to increase in remote Arctic locations.

The O_3 loss rate for 30 March from 11:00 to 13:00, based on the observations, was approximately 3.4 ppbv hr^{-1}. This is much larger than the calculated net O_3 loss rate for the low NO_x simulation of 0.80 ppbv hr^{-1}. The low net O_3 loss rate for the low NO_x simulation could be a result of the constrained model Br_2 mixing ratio not being representative of the ambient air in Barrow at that time, as mentioned previously. If we constrained Br_2 to an estimated concentration lower than what was actually present during that time, we would expect a decreased depletion rate. This belief is supported by a comparison of the BrO data for this time period (discussed later), which is significantly under-simulated by the model. However, this apparent dramatic ozone loss rate could be the observation of an ozone-depleted air mass being transported to the measurement site (Halfacre et al., 2013).

3.3 Model-simulated species vs. OASIS 2009 observations

To further understand both how NO_x decreases the rate of net O_3 loss and affects the bromine chain length, several species that play a crucial role in the bromine cycle were examined. Molecular bromine and its precursors are produced from Reactions (R6) and (R12). The prominent gas-phase recycling reaction is BrO self-reaction (Reaction R3) while the forma-

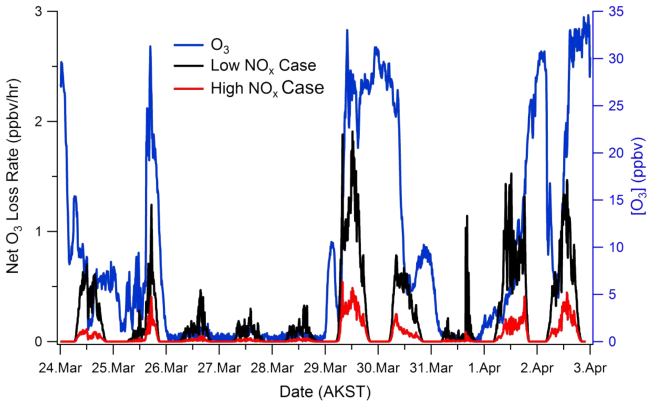

Figure 5. Calculated net O_3 loss rate for the low NO_x and high NO_x simulations, along with the observed O_3 mixing ratios.

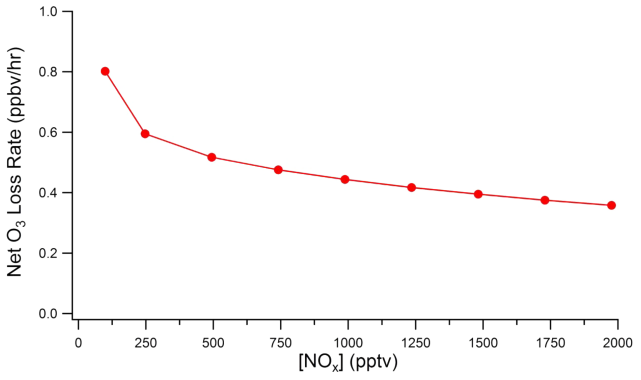

Figure 6. Net O_3 loss rate as a function of the NO_x mixing ratio, for 30 March mid-day (11:00 to 13:00 AKST) conditions.

tion and subsequent deposition of HOBr and $BrONO_2$ leads to heterogeneous reactions that can form Br_2 (Reactions R5–R12). Here we simulated the effect of the low and high NO_x scenarios on BrO, HOBr and $BrONO_2$, and compared the results with the observed mixing ratios during OASIS (Fig. 7a–c). For the majority of the days, simulated BrO for the low NO_x case is close to that observed during OASIS, as expected since low NO_x conditions were typically observed. However, this is not the case for 30 and 31 March, for which the simulated BrO is lower than what was observed during OASIS. This is likely a result of the fact that atmospheric observations for Br_2 on 30 and 31 March were not available, as discussed earlier. For those days the constrained Br_2 was a diurnal average of 29 March and 1 April Br_2 observations. The high NO_x simulation results in a highly suppressed BrO mixing ratio (Fig. 7a), compared to the low NO_x simulation, by more than an order of magnitude throughout the time period. For the high NO_x case, BrO never exceeds 3 pptv, whereas for the low NO_x case, BrO ranges from 2.5 to 25 pptv. For high NO_x days, the BrO mixing ratios are low because of Reactions (R8) and (R10), in which BrO and Br radicals are scavenged by NO_x and converted to temporary termination products.

HOBr responds in similar fashion to changes in NO_x as does BrO, with the low NO_x simulated HOBr being within ± 5 pptv of the OASIS observations while the high NO_x simulated HOBr is much lower. For the most part the low NO_x simulation HOBr is slightly elevated compared to the observed HOBr (26 and 29 March) because the low NO_x simulation has a greater HO_2 mixing ratio compared to the observations.

Figure 7b shows that the high NO_x condition completely suppresses HOBr, and that is what is observed for the high NO_x mixing ratios day, 24 March. However, in contrast to the case for BrO and HOBr, $BrONO_2$ is not suppressed by high NO_x mixing ratios (Fig. 7c), since while increased NO_x suppresses BrO, the rate of R8 is compensated by the increase in NO_x mixing ratios, therefore R8 is largely unchanged. This is shown in Fig. 7C as the $BrONO_2$ mixing ratio is similar for both the high and low NO_x simulations. Additionally, when the model simulated $BrONO_2$ mixing ratio for both NO_x simulations is plotted against the $BrONO_2$ production rate ($k_{BrO+NO_2}[BrO][NO_2]$), it affirms that the $BrONO_2$ mixing ratios follow $k_{BrO+NO_2}[BrO][NO_2]$ (Fig. S2).

3.4 BrO_x and NO_x sinks

It is clear from the discussions above that NO_x influences BrO_x partitioning. The sinks of BrO_x and NO_x were quantified to evaluate their NO_x dependence by including reaction counters on the relevant reactions in the model that convert BrO_x and NO_x to reservoir species. Over the 10-day simulation period for both low and high NO_x cases, NO_x is a significant sink for BrO_x radicals (> 27 %), although for the high NO_x case it contributes more than 50 % (Fig. 4). However, both products of R8 and R10 result in species that can regenerate Br_2. As expected, CH_3CHO plays a major role as a BrO_x sink as well (Shepson et al., 1996), contributing to more than > 35 % in both simulations. Though anthropogenic emissions are known sources of acetaldehyde, observed CH_3CHO mixing ratios were unaffected by Barrow emissions throughout the 10-day simulation period. Thus it is likely that the snowpack is the dominant CH_3CHO source in this study (Grannas et al., 2002). For NO_x, while reactions with HO_2 are important ($\sim$ 20 %), reactions of NO_2 with Br and BrO still represent significant NO_x sinks ($\sim$ 30 %). Peroxynitrates result from an important sink pathway of NO_2, e.g. via Reactions (R17) and (R18), below. Reaction (R17) will be the subject of a separate study.

$$HO_2 + NO_2 \leftrightarrow HO_2NO_2 \quad \text{(R17)}$$

$$CH_3O_2 + NO_2 \leftrightarrow CH_3O_2NO_2 \quad \text{(R18)}$$

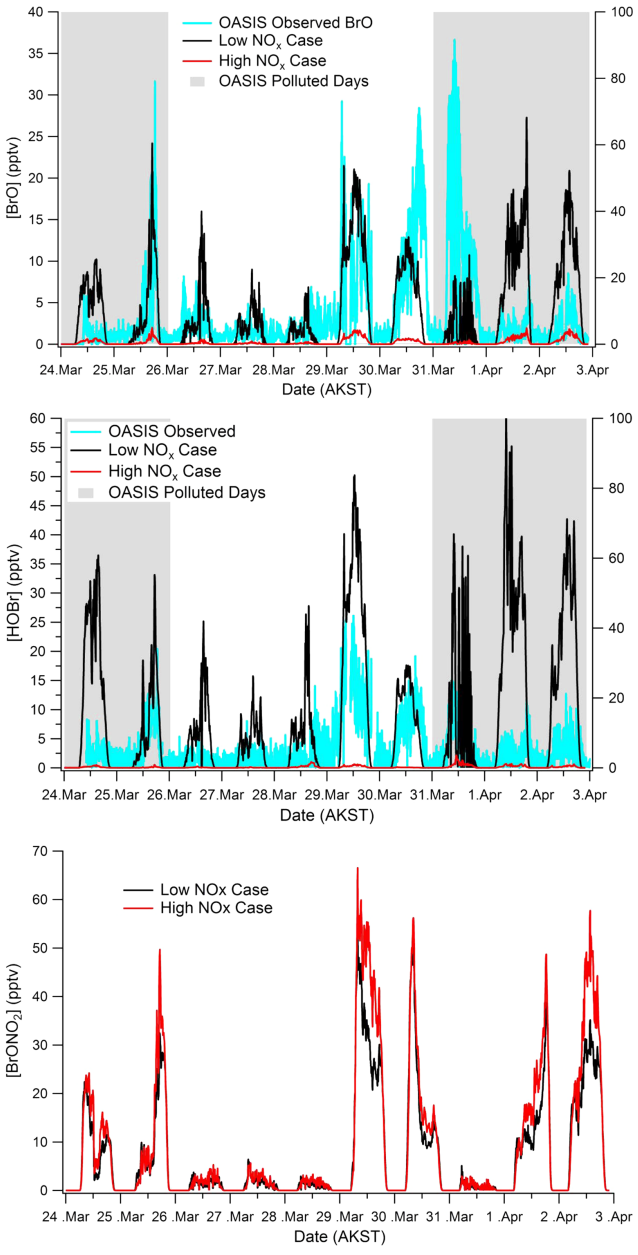

Figure 7. (a) Simulated BrO mixing ratio (low NO_x & high NO_x cases) and the observations during the study period. **(b)** HOBr levels from the model simulations (low NO_x & high NO_x cases) and the observations during the simulation dates. **(c)** $BrONO_2$ mixing ratio from the two simulation cases.

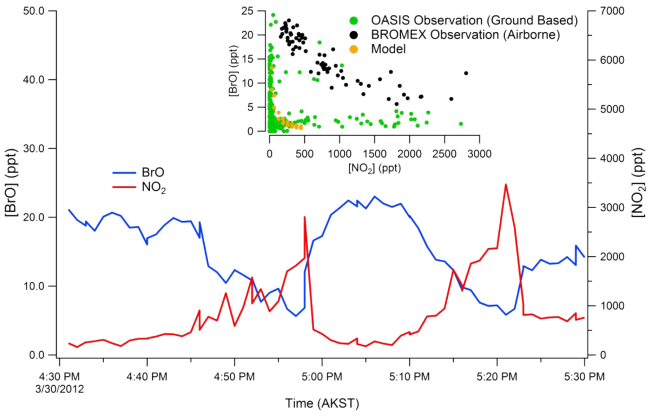

Figure 8. BrO and NO_2 measured mixing ratios via MAX-DOAS during the BROMEX field campaign, near Prudhoe Bay (70° N, 149° W), AK at 700 m above the surface on 30 March 2012. The insert of the NO_2 versus BrO shows the anti-correlation between the two species.

4 BROMEX 2012 field observations

To further examine the interactions between NO_x and reactive bromine, NO_2 and BrO were measured within and around a large combustion plume in the coastal Arctic atmosphere. During the spring 2012 Bromine, Ozone, and Mercury Experiment (BROMEX) field campaign in Barrow, Alaska, airborne measurements of BrO and NO_2 column density (from ∼ 700 m to the surface) were conducted using an aircraft-mounted MAX-DOAS (General et al., 2014) in nadir view. The results for the derived BrO and NO_2 concentrations (from the vertical column density data, assuming a 600 m layer thickness), the average effective mixing ratio from the aircraft to the surface, for a section of a flight on 30 March near Prudhoe Bay, AK, are shown in Fig. 8. Prudhoe Bay is the largest oil field on the North Slope, located ∼ 330 km southeast of Barrow, AK, and produces significant CO_2, NO_x, and CH_4 (Brooks et al., 1997; Jaffe et al., 1995). Anthropogenic emission plumes can easily be observed from the flight by increased NO_2 concentration. This is a good example of the type of point source that is increasing in prevalence in the Arctic (Roiger et al., 2014; Harsem et al., 2011). It can be seen from Fig. 8 that an increase in the concentration of atmospheric NO_2, corresponding to a plume near Prudhoe Bay, coincided with a decrease in the concentration of atmospheric BrO.

The BrO mixing ratio suppression observed during the airborne BROMEX measurement is compared to our model simulations of the OASIS 2009 field observations, in the Fig. 8 insert. To examine the sensitivity in the model and observation of BrO to NO_2, the Br_2 concentration was held constant at 5 pptv throughout the simulation, while NO_2 was varied, for mid-day conditions. The Br_2 concentration was fixed based on the average observed midday (12:00–14:00) concentration during the 10-day simulation time period. NO and NO_2 concentrations were held constant during the entire simulation at a constant ratio of 0.60 for NO_2 : NO, but the absolute magnitude of each concentration was varied between simulations. The data points for both the model and OASIS ground based observations represent data from the time period of 12:00–14:00 AKST.

The model captures the observed distinct sensitivity of BrO to NO_2, decreasing rapidly with increasing NO_2 in the 0–500 pptv NO_2 range. For the BROMEX aircraft data at 600m altitude, while BrO decreases with NO_2, there is more apparent BrO aloft for a given [NO_2]. The relative suppression of BrO at the surface implies a greater BrO_x surface sink, compared to that at 600m. This can be explained from the observations of the BrO_x surface layer sinks expressed in Fig. 4, where a significant sink for BrO_x is Br atom reaction with aldehydes. Given the known snowpack emission source of aldehydes (Grannas et al., 2002; Sumner and Shepson, 1999) and the surface-based character of chlorine chemistry that also produced aldehydes (Tackett et al., 2007), we expect the BrO_x sinks to be enhanced at the surface. The BrO depletion observed during BROMEX is mainly due to Reactions (R8) and (R10) and supports our findings that BrO is suppressed by elevated levels of NO_x (Fig. 7a). Thus, while $BrONO_2$ and $BrNO_2$ can be recycled on surfaces to re-emit Br_2, it seems clear that the net effect of high NO_x mixing ratios is to slow down the overall halogen chain chemistry, as demonstrated in Figures 8 and S1. It should be noted that in very large NO_x plumes O_3 can be removed by the reaction of NO with O_3, as shown in Reaction (R19), although in day light, a photo-steady state will develop from NO_2 photolysis.

$$NO + O_3 \rightarrow NO_2 + O_2 \quad \text{(R19)}$$

If no ozone is present the BrO_x can repartition from BrO towards Br, via photolysis of BrO. During the 30 March 2012 flight the air mass depleted of BrO also had lower ambient O_3 mixing ratios which could explain the BrO depletion.

In Prudhoe Bay, the sources of NO_x are buoyant plumes, located aloft of the surface (smoke stacks), where natural aerosol extinction would be less compared to the surface (Breider et al., 2014). This would limit the availability of surfaces on which $BrONO_2$ could react to re-emit Br_2. However, these NO_x sources also produce aerosols (data not shown; Peters et al., 2011); if these sources continue to increase in number, a shift in the aerosol extinction could occur, providing increased available aerosol surfaces for reaction of $BrONO_2$.

5 Atmospheric implications

It is clear that elevated levels of atmospheric NO_x have a significant effect on the atmospheric chemistry that occurs in the Arctic relating to halogen species. With the possibility of more anthropogenic sources appearing in the Arctic as sea ice area continues to decrease, due to gas and oil exploration and increased shipping traffic, a shift in the atmospheric oxidation capacity and chemical pathways could occur. The main springtime atmospheric oxidizers could change from halogens in the surface layer to a greater contribution from OH via O_3 photolysis, via R20, along with a potential decrease in the frequency of ODEs. Further, open water produces convective mixing, bringing O_3 from aloft down to the surface (Moore et al., 2014). However, the climate change impacts on the Arctic atmosphere and associated chemistry are complex. As multiyear ice retreats, the fraction of first year ice is increasing, leading to more saline ice surfaces. However, the findings of Pratt et al. (2013) indicate that the surface snowpack on the sea ice needs to be acidified for halogen activation to occur, and this likely depends on the depth of the snowpack, which is impacted by snowfall rates and timing, as well as the presence of sea ice. It is now known that snowpack depths in the Beaufort and Chukchi seas have been decreasing at a significant rate (Webster et al., 2014). The acidification of the surface snow also depends on long range transport of acidic species, such as SO_2 and HNO_3 (Worthy et al., 1994), which are likely to change. Moreover, increasing latent heat fluxes (Serreze and Barry, 2011) resulting from more open water will increase the OH production rate in the Arctic because of the humidity dependence of ozone photolysis as shown in Reactions (R20–R22), although a significant increase in humidity would be needed for Reactions (R20–R22) to have an impact on Arctic OH production.

$$O_3 + h\nu \rightarrow O(^1D) + O_2 \quad \text{(R20)}$$

$$O(^1D) + H_2O \rightarrow 2OH \quad \text{(R21)}$$

$$O(^1D) + M \rightarrow O(^3P) + M^* \quad \text{(R22)}$$

Thus, there are multiple competing variables that influence Arctic atmospheric chemistry, and it is surely the case that we will need to continue to integrate simulations with observations to understand the coupling of physical and chemical processes, as the Arctic continues to warm and undergo change at the surface. Finally, we note that the deposition rates and aqueous phase chemistry for the products from the reaction between atmospheric NO_x and halogen radicals are not well known, and fluxes of molecular halogens from Arctic surface snow have not been measured to date. Thus further efforts in this area are necessary to gain a greater understanding of these chemical processes to improve models.

The Supplement related to this article is available online at doi:10.5194/acp-15-10799-2015-supplement.

Acknowledgements. Financial support was provided by the National Science Foundation Office of Polar Programs (ARC-1107695). K. A. Pratt was supported by a National Science Foundation Postdoctoral Fellowship in Polar Regions Research (ARC-1103423). The author thanks the organizers of the OASIS 2009 field campaign along with all the researchers who contributed to the campaign.

Edited by: J. W. Bottenheim

References

Abbatt, J. P. D.: Heterogeneous reaction of HOBr with HBr and HCl on ice surfaces at 228-K, Geophys. Res. Lett., 21, 665–668, doi:10.1029/94gl00775, 1994.

Abbatt, J. P. D., Thomas, J. L., Abrahamsson, K., Boxe, C., Granfors, A., Jones, A. E., King, M. D., Saiz-Lopez, A., Shepson, P. B., Sodeau, J., Toohey, D. W., Toubin, C., von Glasow, R., Wren, S. N., and Yang, X.: Halogen activation via interactions with environmental ice and snow in the polar lower troposphere and other regions, Atmos. Chem. Phys., 12, 6237–6271, doi:10.5194/acp-12-6237-2012, 2012.

Aguzzi, A. and Rossi, M. J.: The kinetics of the heterogeneous reaction of $BrONO_2$ with solid alkali halides at ambient temperature. A comparison with the interaction of $ClONO_2$ on NaCl and KBr, Phys. Chem. Chem. Phys., 1, 4337–4346, doi:10.1039/a904611i, 1999.

Aguzzi, A. and Rossi, M. J.: Heterogeneous hydrolysis and reaction of $BrONO_2$ and Br_2O on pure ice and ice doped with HBr, J. Phys. Chem. A, 106, 5891–5901, doi:10.1021/jp014383e, 2002.

Barrie, L., Bottenheim, J., Schnell, R., Crutzen, P., and Rasmsssen, R.: Ozone Destruction and Photochemical-Reactions at Polar Sunrise in the Lower Arctic Atmosphere, Nature, 334, 138–141, doi:10.1038/334138a0, 1988.

Beine, H., Honrath, R., Domine, F., Simpson, W., and Fuentes, J.: NO_x during background and ozone depletion periods at Alert: Fluxes above the snow surface, J. Geophys. Res.-Atmos., 107, 4584–4595, 10.1029/2002JD002082, 2002.

Breider, T. J., Mickley, L. J., Jacob, D. J., Wang, Q. Q., Fisher, J. A., Chang, R. Y. W., and Alexander, B.: Annual distributions and sources of Arctic aerosol components, aerosol optical depth, and aerosol absorption, J. Geophys. Res.-Atmos., 119, 4107–4124, 2014.

Brooks, S. B., Crawford, T. L., and Oechel, W. C.: Measurement of carbon dioxide emissions plumes from Prudhoe Bay, Alaska oil fields, J. Atmos. Chem., 27, 197–207, doi:10.1023/a:1005890318796, 1997.

Burkholder, J. B. and Orlando, J. J.: UV absorption cross-sections of cis-BrONO, Chem. Phys. Lett., 317, 603–608, doi:10.1016/s0009-2614(99)01412-8, 2000.

Cao, L., Sihler, H., Platt, U., and Gutheil, E.: Numerical analysis of the chemical kinetic mechanisms of ozone depletion and halogen release in the polar troposphere, Atmos. Chem. Phys., 14, 3771–3787, doi:10.5194/acp-14-3771-2014, 2014.

Corbett, J. J., Lack, D. A., Winebrake, J. J., Harder, S., Silberman, J. A., and Gold, M.: Arctic shipping emissions inventories and future scenarios, Atmos. Chem. Phys., 10, 9689–9704, doi:10.5194/acp-10-9689-2010, 2010.

Domine, F., Bock, J., Voisin, D., and Donaldson, D. J.: Can We Model Snow Photochemistry?, Problems with the Current Approaches, J. Phys. Chem. A, 117, 4733–4749, doi:10.1021/jp3123314, 2013.

Dubowski, Y., Colussi, A. J., and Hoffmann, M. R.: Nitrogen dioxide release in the 302 nm band photolysis of spray-frozen aqueous nitrate solutions. Atmospheric implications, J. Phys. Chem. A, 105, 4928–4932, doi:10.1021/jp0042009, 2001.

Dubowski, Y., Colussi, A. J., Boxe, C., and Hoffmann, M. R.: Monotonic increase of nitrite yields in the photolysis of nitrate in ice and water between 238 and 294 K, J. Phys. Chem. A, 106, 6967–6971, doi:10.1021/jp0142942, 2002.

Evans, M. J., Jacob, D. J., Atlas, E., Cantrell, C. A., Eisele, F., Flocke, F., Fried, A., Mauldin, R. L., Ridley, B. A., Wert, B., Talbot, R., Blake, D., Heikes, B., Snow, J., Walega, J., Weinheimer, A. J., and Dibb, J.: Coupled evolution of BrO_x-ClO_x-HO_x-NO_x chemistry during bromine-catalyzed ozone depletion events in the arctic boundary layer, J. Geophys. Res.-Atmos., 108, 12 8368–8379, doi:10.1029/2002jd002732, 2003.

Fan, S. and Jacob, D.: Surface Ozone Depletion in Arctic Spring Sustained by Bromine Reactions on Aerosols, Nature, 359, 522–524, doi:10.1038/359522a0, 1992.

Foster, K., Plastridge, R., Bottenheim, J., Shepson, P., Finlayson-Pitts, B., and Spicer, C.: The role of Br-2 and BrCl in surface ozone destruction at polar sunrise, Science, 291, 471–474, doi:10.1126/science.291.5503.471, 2001.

General, S., Pöhler, D., Sihler, H., Bobrowski, N., Frieß, U., Zielcke, J., Horbanski, M., Shepson, P. B., Stirm, B. H., Simpson, W. R., Weber, K., Fischer, C., and Platt, U.: The Heidelberg Airborne Imaging DOAS Instrument (HAIDI) – a novel imaging DOAS device for 2-D and 3-D imaging of trace gases and aerosols, Atmos. Meas. Tech., 7, 3459–3485, doi:10.5194/amt-7-3459-2014, 2014.

Grannas, A., Shepson, P., Guimbaud, C., Sumner, A., Albert, M., Simpson, W., Domine, F., Boudries, H., Bottenheim, J., Beine, H., Honrath, R., and Zhou, X.: A study of photochemical and physical processes affecting carbonyl compounds in the Arctic atmospheric boundary layer, Atmos. Environ., 36, 2733–2742, doi:10.1016/S1352-2310(02)00134-6, 2002.

Grannas, A. M., Jones, A. E., Dibb, J., Ammann, M., Anastasio, C., Beine, H. J., Bergin, M., Bottenheim, J., Boxe, C. S., Carver, G., Chen, G., Crawford, J. H., Dominé, F., Frey, M. M., Guzmán, M. I., Heard, D. E., Helmig, D., Hoffmann, M. R., Honrath, R. E., Huey, L. G., Hutterli, M., Jacobi, H. W., Klán, P., Lefer, B., McConnell, J., Plane, J., Sander, R., Savarino, J., Shepson, P. B., Simpson, W. R., Sodeau, J. R., von Glasow, R., Weller, R., Wolff, E. W., and Zhu, T.: An overview of snow photochemistry: evidence, mechanisms and impacts, Atmos. Chem. Phys., 7, 4329–4373, doi:10.5194/acp-7-4329-2007, 2007.

Halfacre, J. W., Knepp, T. N., Shepson, P. B., Stephens, C. R., Pratt, K. A., Li, B., Peterson, P. K., Walsh, S. J., Simpson, W. R., Matrai, P. A., Bottenheim, J. W., Netcheva, S., Perovich, D. K., and Richter, A.: Temporal and spatial characteristics of ozone depletion events from measurements in the Arctic, Atmos. Chem. Phys. Discuss., 13, 30233–30285, doi:10.5194/acpd-13-30233-2013, 2013.

Hanson, D.: Reactivity of $BrONO_2$ and HOBr on sulfuric acid solutions at low temperatures, J. Geophys. Res.-Atmos., 108, 4239–4249, doi:10.1029/2002JD002519, 2003.

Hanson, D., Ravishankara, A., and Lovejoy, E.: Reaction of $BrONO_2$ with H_2O on submicron sulfuric acid aerosol and the implications for the lower stratosphere, J. Geophys. Res.-Atmos., 101, 9063–9069, doi:10.1029/96JD00347, 1996.

Harsem, O., Eide, A., and Heen, K.: Factors influencing future oil and gas prospects in the Arctic, Energ. Policy, 39, 8037–8045, doi:10.1016/j.enpol.2011.09.058, 2011.

Hausmann, M. and Platt, U.: Spectroscopic measurement of bromine oxide and ozone in the high arctic during Polar Sunrise Experiment 1992, J. Geophys. Res.-Atmos., 99, 25399–25413, doi:10.1029/94jd01314, 1994.

Honrath, R. E., Peterson, M. C., Guo, S., Dibb, J. E., Shepson, P. B., and Campbell, B.: Evidence of NO_x production within or upon ice particles in the Greenland snowpack, Geophys. Res. Lett., 26, 695–698, doi:10.1029/1999gl900077, 1999.

Honrath, R. E., Guo, S., Peterson, M. C., Dziobak, M. P., Dibb, J. E., and Arsenault, M. A.: Photochemical production of gas phase NO_x from ice crystal NO_3, J. Geophys. Res.-Atmos., 105, 24183–24190, doi:10.1029/2000jd900361, 2000.

Honrath, R. E., Lu, Y., Peterson, M. C., Dibb, J. E., Arsenault, M. A., Cullen, N. J., and Steffen, K.: Vertical fluxes of NO_x, HONO, and HNO_3 above the snowpack at Summit, Greenland, Atmos. Environ., 36, 2629–2640, doi:10.1016/s1352-2310(02)00132-2, 2002.

Huff, A. K. and Abbatt, J. P. D.: Kinetics and product yields in the heterogeneous reactions of HOBr with ice surfaces containing NaBr and NaCl, J. Phys. Chem. A, 106, 5279–5287, doi:10.1021/jp014296m, 2002.

Impey, G., Shepson, P., Hastie, D., Barrie, L., and Anlauf, K.: Measurements of photolyzable chlorine and bromine during the Polar sunrise experiment 1995, J. Geophys. Res.-Atmos., 102, 16005–16010, doi:10.1029/97JD00851, 1997.

Jaffe, D. A., Honrath, R. E., Furness, D., Conway, T. J., Dlugokencky, E., and Steele, L. P.: A determination of the CH_4, NO_x, and CO_2 emissions from the Prudhoe Bay, Alaska oil development, J. Atmos. Chem., 20, 213–227, doi:10.1007/bf00694494, 1995.

Liao, J., Huey, L., Tanner, D., Flocke, F., Orlando, J., Neuman, J., Nowak, J., Weinheimer, A., Hall, S., Smith, J., Fried, A., Staebler, R., Wang, Y., Koo, J., Cantrell, C., Weibring, P., Walega, J., Knapp, D., Shepson, P., and Stephens, C.: Observations of inorganic bromine (HOBr, BrO, and Br-2) speciation at Barrow, Alaska, in spring 2009, J. Geophys. Res.-Atmos., 117, D00R16, doi:10.1029/2011JD016641, 2012.

McConnell, J., Henderson, G., Barrie, L., Bottenheim, J., Niki, H., Langford, C., and Templeton, E.: Photochemical Bromine Production Implicated in Arctic Boundary-Layer Ozone Depletion, Nature, 355, 150–152, doi:10.1038/355150a0, 1992.

Michalowski, B., Francisco, J., Li, S., Barrie, L., Bottenheim, J., and Shepson, P.: A computer model study of multiphase chemistry in the Arctic boundary layer during polar sunrise, J. Geophys. Res.-Atmos., 105, 15131–15145, doi:10.1029/2000JD900004, 2000.

Moore, C. W., Obrist, D., Steffen, A., Staebler, R. M., Douglas, T. A., Richter, A., and Nghiem, S. V.: Convective forcing of mercury and ozone in the Arctic boundary layer induced by leads in sea ice, Nature, 506, 81–84, doi:10.1038/nature12924, 2014.

Morin, S., Savarino, J., Bekki, S., Gong, S., and Bottenheim, J. W.: Signature of Arctic surface ozone depletion events in the isotope anomaly ($\delta^{17}O$) of atmospheric nitrate, Atmos. Chem. Phys., 7, 1451–1469, doi:10.5194/acp-7-1451-2007, 2007.

Morin, S., Erbland, J., Savarino, J., Domine, F., Bock, J., Friess, U., Jacobi, H. W., Sihler, H., and Martins, J. M. F.: An isotopic view on the connection between photolytic emissions of NO_x from the Arctic snowpack and its oxidation by reactive halogens, J. Geophys. Res.-Atmos., 117, 15 D00R08, doi:10.1029/2011jd016618, 2012.

Muthuramu, K., Shepson, P. B., Bottenheim, J. W., Jobson, B. T., Niki, H., and Anlauf, K. G.: Relationships Between Organic Nitrates and Surface Ozone Destruction During Polar Sunrise Experiment 1992, J. Geophys. Res.-Atmos., 99, 25369–25378, doi:10.1029/94jd01309, 1994.

Orlando, J. J. and Burkholder, J. B.: Identification of BrONO as the major product in the gas-phase reaction of Br with NO_2, J. Phys. Chem. A, 104, 2048–2053, doi:10.1021/jp993713g, 2000.

Peters, G. P., Nilssen, T. B., Lindholt, L., Eide, M. S., Glomsrød, S., Eide, L. I., and Fuglestvedt, J. S.: Future emissions from shipping and petroleum activities in the Arctic, Atmos. Chem. Phys., 11, 5305–5320, doi:10.5194/acp-11-5305-2011, 2011.

Pohler, D., Vogel, L., Friess, U., and Platt, U.: Observation of halogen species in the Amundsen Gulf, Arctic, by active long-path differential optical absorption spectroscopy, P. Natl. Acad. Sci. USA, 107, 6582–6587, doi:10.1073/pnas.0912231107, 2010.

Pratt, K., Custard, K., Shepson, P., Douglas, T., Pohler, D., General, S., Zielcke, J., Simpson, W., Platt, U., Tanner, D., Huey, L., Carlsen, M., and Stirm, B.: Photochemical production of molecular bromine in Arctic surface snowpacks, Nat. Geosci., 6, 351–356, doi:10.1038/NGEO1779, 2013.

Ridley, B., Walega, J., Montzka, D., Grahek, F., Atlas, E., Flocke, F., Stroud, V., Deary, J., Gallant, A., Boudries, H., Bottenheim, J., Anlauf, K., Worthy, D., Sumner, A., Splawn, B., and Shepson, P.: Is the Arctic surface layer a source and sink of NO_x in winter/spring?, J. Atmos. Chem., 36, 1–22, doi:10.1023/A:1006301029874, 2000.

Ridley, B. A. and Orlando, J. J.: Active nitrogen in surface ozone depletion events at alert during spring 1998, J. Atmos. Chem., 44, 1–22, doi:10.1023/a:1022188822920, 2003.

Roiger, A., Thomas, J. L., Schlager, H., Law, K. S., Kim, J., Schäfler, A., Weinzierl, B., Dahlkötter, F., Krisch, I., Marelle, L., Minikin, A., Raut, J. C., Reiter, A., Rose, M., Scheibe, M., Stock, P., Baumann, R., Bouarar, I., Clerbaux, C., George, M., Onishi, T., and Flemming, J.: "Quantifying emerging local anthropogenic emissions in the Arctic region: the ACCESS aircraft campaign experiment", B. Am. Meteorol. Soc., 96, 441–460, doi:10.1175/BAMS-D-13-00169.1, 2014.

Serreze, M. C. and Barry, R. G.: Processes and impacts of Arctic amplification: A research synthesis, Global Planet. Change, 77, 85–96, doi:10.1016/j.gloplacha.2011.03.004, 2011.

Shepson, P. B., Sirju, A. P., Hopper, J. F., Barrie, L. A., Young, V., Niki, H., and Dryfhout, H.: Sources and sinks of carbonyl compounds in the arctic ocean boundary layer: Polar ice floe experiment, J. Geophys. Res.-Atmos., 101, 21081–21089, doi:10.1029/96jd02032, 1996.

Simpson, W. R., von Glasow, R., Riedel, K., Anderson, P., Ariya, P., Bottenheim, J., Burrows, J., Carpenter, L. J., Frieß, U., Goodsite, M. E., Heard, D., Hutterli, M., Jacobi, H.-W., Kaleschke, L., Neff, B., Plane, J., Platt, U., Richter, A., Roscoe, H., Sander, R., Shepson, P., Sodeau, J., Steffen, A., Wagner, T., and Wolff, E.: Halogens and their role in polar boundary-layer ozone depletion, Atmos. Chem. Phys., 7, 4375–4418, doi:10.5194/acp-7-4375-2007, 2007.

Sumner, A. L. and Shepson, P. B.: Snowpack production of formaldehyde and its effect on the Arctic troposphere, Nature, 398, 230–233, 1999.

Tackett, P., Cavender, A., Keil, A., Shepson, P., Bottenheim, J., Morin, S., Deary, J., Steffen, A., and Doerge, C.: A study of the vertical scale of halogen chemistry in the Arctic troposphere during Polar Sunrise at Barrow, Alaska, J. Geophys. Res.-Atmos., 112, D07306, doi:10.1029/2006JD007785, 2007.

Tang, T. and McConnell, J.: Autocatalytic release of bromine from Arctic snow pack during polar sunrise, Geophys. Res. Lett., 23, 2633–2636, doi:10.1029/96GL02572, 1996.

Thomas, J. L., Dibb, J. E., Huey, L. G., Liao, J., Tanner, D., Lefer, B., von Glasow, R., and Stutz, J.: Modeling chemistry in and above snow at Summit, Greenland – Part 2: Impact of snowpack chemistry on the oxidation capacity of the boundary layer, Atmos. Chem. Phys., 12, 6537–6554, doi:10.5194/acp-12-6537-2012, 2012.

Thompson, C. R., Shepson, P. B., Liao, J., Huey, L. G., Apel, E. C., Cantrell, C. A., Flocke, F., Orlando, J., Fried, A., Hall, S. R., Hornbrook, R. S., Knapp, D. J., Mauldin III, R. L., Montzka, D. D., Sive, B. C., Ullmann, K., Weibring, P., and Weinheimer, A.: Interactions of bromine, chlorine, and iodine photochemistry during ozone depletions in Barrow, Alaska, Atmos. Chem. Phys., 15, 9651–9679, doi:10.5194/acp-15-9651-2015, 2015.

Thorn, R. P., Daykin, E. P., and Wine, P. H.: Kinetics of the $BrO+NO_2$ association reaction. Temperature and pressure dependence in the falloff regime, Int. J. Chem. Kinet., 25, 521–537, doi:10.1002/kin.550250703, 1993.

Toyota, K., Dastoor, A. P., and Ryzhkov, A.: Air-snowpack exchange of bromine, ozone and mercury in the springtime Arctic simulated by the 1-D model PHANTAS – Part 2: Mercury and its speciation, Atmos. Chem. Phys. Discuss., 13, 22151-22220, doi:10.5194/acpd-13-22151-2013, 2013.

Toyota, K., Dastoor, A. P., and Ryzhkov, A.: Air-snowpack exchange of bromine, ozone and mercury in the springtime Arctic simulated by the 1-D model PHANTAS – Part 2: Mercury and its speciation, Atmos. Chem. Phys., 14, 4135–4167, doi:10.5194/acp-14-4135-2014, 2014.

Villena, G., Wiesen, P., Cantrell, C., Flocke, F., Fried, A., Hall, S., Hornbrook, R., Knapp, D., Kosciuch, E., Mauldin, R., McGrath, J., Montzka, D., Richter, D., Ullmann, K., Walega, J., Weibring, P., Weinheimer, A., Staebler, R., Liao, J., Huey, L., and Kleffmann, J.: Nitrous acid (HONO) during polar spring in Barrow, Alaska: A net source of OH radicals?, J. Geophys. Res.-Atmos., 116, D00R07, doi:10.1029/2011JD016643, 2011.

Vogt, R., Crutzen, P., and Sander, R.: A mechanism for halogen release from sea-salt aerosol in the remote marine boundary layer, Nature, 383, 327–330, doi:10.1038/383327a0, 1996.

von Glasow, R., Sander, R., Bott, A., and Crutzen, P.: Modeling halogen chemistry in the marine boundary layer – 1. Cloud-free MBL, J. Geophys. Res.-Atmos., 107, 4341–4356, doi:10.1029/2001JD000942, 2002.

Webster, M. A., Rigor, I. G., Nghiem, S. V., Kurtz, N. T., Farrell, S. L., Perovich, D. K., and Sturm, M.: Interdecadal changes in snow depth on Arctic sea ice, J. Geophys. Res.-Oceans, 119, 5395–5406, doi:10.1002/2014jc009985, 2014.

Wennberg, P.: Atmospheric chemistry – Bromine explosion, Nature, 397, 299 299–301, doi:10.1038/16805, 1999.

Worthy, D. E. J., Trivett, N. B. A., Hopper, J. F., Bottenheim, J. W., and Levin, I.: Analysis of long-range transport events at Alert, Northwest Territories, during the Polar Sunrise Experiment, J. Geophys. Res.-Atmos., 99, 25329–25344, doi:10.1029/94jd01209, 1994.